

Representation of Crystallographic Subperiodic Groups in Clifford's Geometric Algebra

Eckhard Hitzer and Daisuke Ichikawa

Soli Deo Gloria.

Abstract. This paper explains how, following the representation of 3D crystallographic space groups in Clifford's geometric algebra, it is further possible to similarly represent the 162 so called subperiodic groups of crystallography in Clifford's geometric algebra. A new compact geometric algebra group representation symbol is constructed, which allows to read off the complete set of geometric algebra generators. For clarity moreover the chosen generators are stated explicitly. The group symbols are based on the representation of point groups in geometric algebra by versors (Clifford monomials, Lipschitz elements).

Mathematics Subject Classification (2010). Primary 20H15; Secondary 15A66.

Keywords. Subperiodic groups, Clifford's geometric algebra, versor representation, frieze groups, rod groups, layer groups.

1. Introduction

Crystals are fundamentally periodic geometric arrangements of atoms, ions or molecules. The directed distance between two such elements is a Euclidean vector in \mathbb{R}^3 . Intuitively all symmetry properties of crystals depend on these vectors. Indeed, the geometric product of vectors [6] combined with the conformal model of 3D Euclidean space [10, 13, 25, 26, 28] yields an algebra fully expressing crystal point and space groups [8, 11, 14, 15]. Two successive reflections at (non-) parallel planes express (rotations) translations, etc. [3, 4]. This leads to a 1:1 correspondence of geometric objects and symmetry operators [21] with vectors and their products, ideal for creating a suite of interactive visualizations using CLUCalc [29] and OpenGL [15, 16, 18–20]. Independently it has been shown that the coincidence site lattice transformation groups, important for modeling crystalline interfaces and grain boundaries, can be completely determined by coincidence symmetry reflections through hyperplanes orthogonal to lattice vectors [32, 33, 37, 38].

For material science the subperiodic space groups [23] in 2D and 3D with only one or two degrees of freedom for translations are also of great interest. This

article introduces a new algebraic representation for all subperiodic groups of crystallography, including, for the first time, a complete highly compact multiplicative presentation of the generators for each group. By presentation we mean an explicit representation of group elements. We also introduce a compact new system of subperiodic group symbols that enables one to write down the generators for each group directly from the group symbol. Earlier initial work, reported in [19], is thus completed.

We begin in Section 2 by explaining the representation of point and space groups in conformal geometric algebra. Then in Section 3 we show how to construct a new compact geometric algebra group representation symbol for subperiodic space groups (frieze groups, rod groups and layer groups), which allows to read off the complete set of geometric algebra generators. For clarity we moreover state explicitly what generators are chosen.

2. Point groups and space groups in Clifford's geometric algebra

2.1. Cartan-Dieudonné and Clifford's geometric algebra

Clifford's associative geometric product [2,6] of two vectors simply adds the (symmetric) inner product to the (anti-symmetric) outer product of Grassmann

$$\mathbf{ab} = \mathbf{a} \cdot \mathbf{b} + \mathbf{a} \wedge \mathbf{b}. \quad (2.1)$$

The mathematical meaning of the left and right side of (2.1) is clear from applying the geometric product to the n orthonormal basis vectors $\{\mathbf{e}_1, \dots, \mathbf{e}_n\}$ of the underlying vector space $\mathbb{R}^{p,q}, n = p + q$. We thus have

$$\mathbf{e}_k \mathbf{e}_k = \mathbf{e}_k \cdot \mathbf{e}_k = +1, \quad \mathbf{e}_k \wedge \mathbf{e}_k = 0, \quad 1 \leq k \leq p, \quad (2.2)$$

$$\mathbf{e}_k \mathbf{e}_k = \mathbf{e}_k \cdot \mathbf{e}_k = -1, \quad \mathbf{e}_k \wedge \mathbf{e}_k = 0, \quad p+1 \leq k \leq n, \quad (2.3)$$

$$\mathbf{e}_k \mathbf{e}_l = -\mathbf{e}_l \mathbf{e}_k = \mathbf{e}_k \wedge \mathbf{e}_l, \quad \mathbf{e}_k \cdot \mathbf{e}_l = 0, \quad l \neq k, 1 \leq k, l \leq n. \quad (2.4)$$

Under this product parallel vectors commute and perpendicular vectors anti-commute

$$\mathbf{ax}_{\parallel} = \mathbf{x}_{\parallel} \mathbf{a}, \quad \mathbf{ax}_{\perp} = -\mathbf{x}_{\perp} \mathbf{a}. \quad (2.5)$$

This allows to write the *reflection* of a vector \mathbf{x} at a hyperplane through the origin with normal \mathbf{a} as (see left side of Fig. 1)

$$\mathbf{x}' = -\mathbf{a}^{-1} \mathbf{x} \mathbf{a}, \quad \mathbf{a}^{-1} = \frac{\mathbf{a}}{\mathbf{a}^2} \quad \mathbf{a}^{-1} \mathbf{a} = \mathbf{a} \mathbf{a}^{-1} = 1. \quad (2.6)$$

We can prove (2.6) by beginning with the expression of the reflected vector (see left side of Fig. 1 for the meaning of \mathbf{x}_{\parallel} and \mathbf{x}_{\perp} relative to \mathbf{a}):

$$\begin{aligned} \mathbf{x}' &= -\mathbf{x}_{\parallel} + \mathbf{x}_{\perp} = -\mathbf{a}^{-1} \mathbf{x} \mathbf{a}_{\parallel} + \mathbf{a}^{-1} \mathbf{x} \mathbf{a}_{\perp} = -\mathbf{a}^{-1} \mathbf{x}_{\parallel} \mathbf{a} - \mathbf{a}^{-1} \mathbf{x}_{\perp} \mathbf{a} \\ &= -\mathbf{a}^{-1} (\mathbf{x}_{\parallel} + \mathbf{x}_{\perp}) \mathbf{a} = -\mathbf{a}^{-1} \mathbf{x} \mathbf{a}, \end{aligned} \quad (2.7)$$

where we have used (2.5) for the third equality.

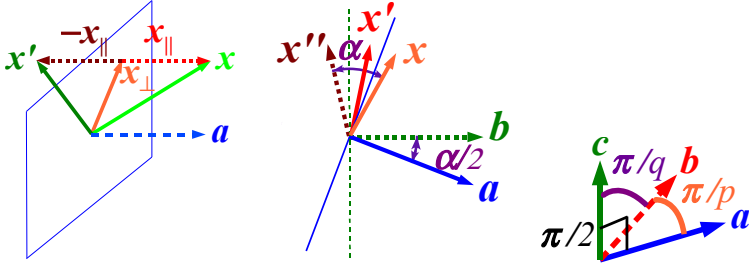


FIGURE 1. Left: Reflection at a hyperplane normal to \mathbf{a} . Center: Rotation generated by two successive reflections at hyperplanes normal to \mathbf{a}, \mathbf{b} by twice the angle $\angle(\mathbf{a}, \mathbf{b})$. Right: Angular relations of pairs of geometric cell vectors of $\mathbf{a}, \mathbf{b}, \mathbf{c}$: $\angle(\mathbf{a}, \mathbf{b}) = \pi/p$, $\angle(\mathbf{b}, \mathbf{c}) = \pi/q$, $\angle(\mathbf{a}, \mathbf{c}) = \pi/2$, $p, q \in \{1, 2, 3, 4, 6\}$.

The composition of two reflections at hyperplanes, whose normal vectors \mathbf{a}, \mathbf{b} subtend the angle $\alpha/2$, yields a rotation around the intersection of the two hyperplanes (see center of Fig. 1) by α

$$\mathbf{x}'' = (\mathbf{ab})^{-1} \mathbf{x} \mathbf{ab}, \quad (\mathbf{ab})^{-1} = \mathbf{b}^{-1} \mathbf{a}^{-1}. \quad (2.8)$$

Continuing with a third reflection at a hyperplane with normal \mathbf{c} according to the Cartan–Dieudonné theorem¹ [1, 5, 34, 36] yields rotary reflections (equivalent to rotary inversions with angle $\alpha - \pi$)

$$\mathbf{x}' = -(\mathbf{abc})^{-1} \mathbf{x} \mathbf{abc}, \quad (2.9)$$

and inversions

$$\mathbf{x}'' = -i^{-1} \mathbf{x} i, \quad i \doteq \mathbf{a} \wedge \mathbf{b} \wedge \mathbf{c}, \quad (2.10)$$

where \doteq means equality up to non-zero scalar factors (which cancel out in (2.11)). In general the geometric product $S = \mathbf{abc}\dots$ of k , normal vectors corresponds to the composition of reflections to all symmetry transformations [11, 12] of two-dimensional (2D) and 3D point groups², which describe the symmetry of crystal cells,

$$\mathbf{x}' = (-1)^k S^{-1} \mathbf{x} S = \widehat{S}^{-1} \mathbf{x} \widehat{S} = S^{-1} \mathbf{x} \widehat{S}, \quad (2.11)$$

where $\widehat{S} = (-1)^k S$ is the *grade involution* or *main involution* in Clifford's geometric algebra (GA). We call the product of invertible vectors S in (2.11) *versor* [7, 12, 21, 25], but the names *Clifford monomial* of invertible vectors, *Clifford group element*, or *Lipschitz group element* are equally in use [25, 27].

¹The decomposition of space group transformations in the conformal model $Cl(p+1, q+1)$ according to the Cartan–Dieudonné theorem is always possible, though it is clearly not unique, since, e.g., any two Euclidean vectors in the same plane, which enclose the angle $\alpha/2$ will generate the rotation in that plane by the angle α . Different choices of lattice vectors allow therefore still to generate the same space group. For example, in the hexagon of Fig. 2, vector \mathbf{a} could obviously be replaced by any of the other five side vectors and \mathbf{b} then by a vector to a respective neighboring vertex.

²Note, that a (geometric) crystal class contains crystals that share the same type of point group. Therefore, the same symbol is used for both point group and crystal class, but there is a fundamental ontological difference between the two concepts.

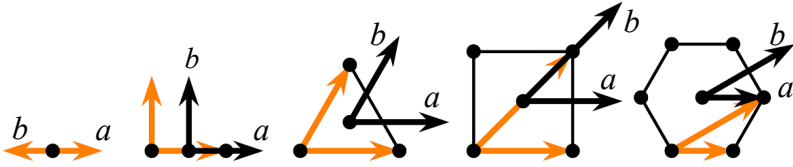


FIGURE 2. Regular polygons ($p = 1, 2, 3, 4, 6$) and point group generating vectors \mathbf{a}, \mathbf{b} subtending angles π/p attached to figure center.

TABLE 1. Geometric and international notation for 2D point groups.

Crystal system	Oblique	Rectangular	Trigonal	Square	Hexagonal					
geometric	$\bar{1}$	$\bar{2}$	1	2	3	$\bar{3}$	4	$\bar{4}$	6	$\bar{6}$
international	1	2	m	2mm	3m	3	4mm	4	6mm	6

TABLE 2. Geometric 3D point group symbols [11] and generators with $\theta_{\mathbf{a},\mathbf{b}} = \pi/p$, $\theta_{\mathbf{b},\mathbf{c}} = \pi/q$, $\theta_{\mathbf{a},\mathbf{c}} = \pi/2$, $p, q \in \{1, 2, 3, 4, 6\}$, see the right side of Fig. 1.

Symbols	$p = 1$	$p \neq 1$	\bar{p}	pq	$\bar{p}q$	$p\bar{q}$	$\bar{p}\bar{q}$	\overline{pq}
Generators	\mathbf{a}	\mathbf{a}, \mathbf{b}	\mathbf{ab}	$\mathbf{a}, \mathbf{b}, \mathbf{c}$	\mathbf{ab}, \mathbf{c}	\mathbf{a}, \mathbf{bc}	\mathbf{ab}, \mathbf{bc}	\mathbf{abc}

2.2. Two dimensional point groups

2D point groups [11] are generated by multiplying vectors selected [14, 15] as in Fig. 2. The index p can be used to denote these groups as in Table 1. For example the hexagonal point group is given by multiplying its two generating vectors \mathbf{a}, \mathbf{b}

$$6 = \{\mathbf{a}, \mathbf{b}, R = \mathbf{ab}, R^2, R^3, R^4, R^5, R^6 \doteq -1, \\ \mathbf{a}R^2, \mathbf{b}R^2, \mathbf{a}R^4, \mathbf{b}R^4\}. \quad (2.12)$$

The rotation subgroups are denoted with bars, e.g. $\bar{6}$. The identities $\mathbf{a}^2 \doteq \mathbf{b}^2 \doteq 1$ and $R^6 \doteq -1$ directly correspond to relations in the group presentation [35] of 6.

2.3. Three dimensional point groups

The selection of three vectors $\mathbf{a}, \mathbf{b}, \mathbf{c}$ from each crystal cell [11, 16] for generating (cf. Table 2) 3D point groups are indicated in Figs. 3 and 4.

The selection of three vectors $\mathbf{a}, \mathbf{b}, \mathbf{c}$, see the right side of Fig. 1, from each crystal cell [11, 14, 15] for generating all 3D point groups is indicated in Figs. 3 and 4. Using $\angle(\mathbf{a}, \mathbf{b})$ and $\angle(\mathbf{b}, \mathbf{c})$ we can denote all 32 3D point groups (and their associated crystal classes) as in Table 2. For example the monoclinic point groups

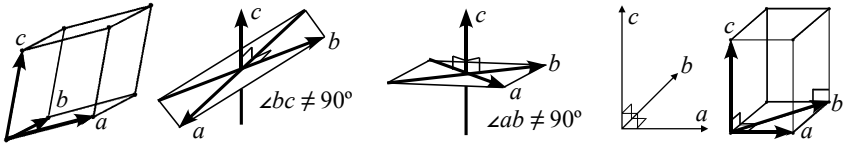


FIGURE 3. From left to right: Triclinic, monoclinic inclined, monoclinic orthogonal, orthorhombic, and tetragonal cell vectors $\mathbf{a}, \mathbf{b}, \mathbf{c}$ for rod and layer groups.

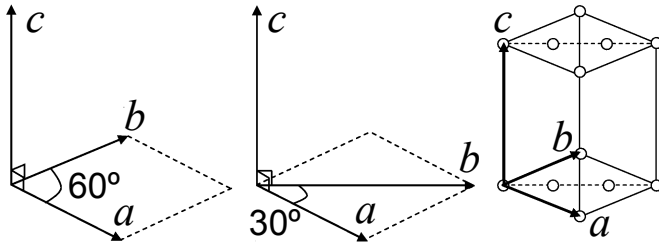


FIGURE 4. Generating vectors $\mathbf{a}, \mathbf{b}, \mathbf{c}$ of cell choices for trigonal and hexagonal crystal systems for 3D rod and layer groups. Left: a hexagonal primitive (hP) cell. Center: an ortho-hexagonal C -centered cell (oC). Right: a hexagonal H -centered cell (hH) with Bravais symbol in the nomenclature: H or h .

are then (int. symbols of Hermann-Mauguin: 2/m, m and 2, respectively)

$$2\bar{2} = \{\mathbf{c}, R = \mathbf{a} \wedge \mathbf{b} = i\mathbf{c}, i = \mathbf{c}R, 1\}, \quad (2.13)$$

$$1 = \{\mathbf{c}, 1\}, \quad (2.14)$$

$$\bar{2} = \{i\mathbf{c}, 1\}. \quad (2.15)$$

2.4. Space groups

The smooth composition with translations is best done in the conformal model [10, 13, 25, 26, 28] of Euclidean space (in the GA of $\mathbb{R}^{4,1}$), which adds two null-vector dimensions for the origin \mathbf{e}_0 and infinity \mathbf{e}_∞ such that

$$X = \mathbf{x} + \frac{1}{2}\mathbf{x}^2\mathbf{e}_\infty + \mathbf{e}_0, \quad (2.16)$$

$$\mathbf{e}_0^2 = \mathbf{e}_\infty^2 = X^2 = 0, \quad (2.17)$$

$$X \cdot \mathbf{e}_\infty = -1. \quad (2.18)$$

The $+\mathbf{e}_0$ term integrates projective geometry, and the $+\frac{1}{2}\mathbf{x}^2\mathbf{e}_\infty$ term ensures $X^2 = 0$. The inner product of two conformal points gives their Euclidean distance and therefore a plane m equidistant from two points A, B as

$$X \cdot A = -\frac{1}{2}(\mathbf{x} - \mathbf{a})^2 \Rightarrow X \cdot (A - B) = 0, \quad (2.19)$$

$$m = A - B \propto \mathbf{p} - d\mathbf{e}_\infty, \quad (2.20)$$

TABLE 3. Computing with reflections and translations. The vectors \mathbf{a}, \mathbf{b} are pictured in Fig. 2.

$\angle(\mathbf{a}, \mathbf{b})$	180°	90°	60°	45°	30°
$T_{\mathbf{a}} \mathbf{b} =$	$\mathbf{b} T_{-\mathbf{a}}$	$\mathbf{b} T_{\mathbf{a}}$	$\mathbf{b} T_{\mathbf{a}-\mathbf{b}}$	$\mathbf{b} T_{\mathbf{a}-\mathbf{b}}$	$\mathbf{b} T_{\mathbf{a}-\mathbf{b}}$
$T_{\mathbf{b}} \mathbf{a} =$	$\mathbf{a} T_{-\mathbf{b}}$	$\mathbf{a} T_{\mathbf{b}}$	$\mathbf{a} T_{\mathbf{b}-\mathbf{a}}$	$\mathbf{a} T_{\mathbf{b}-2\mathbf{a}}$	$\mathbf{a} T_{\mathbf{b}-3\mathbf{a}}$

where \mathbf{p} is a unit normal to the plane and d its signed scalar distance from the origin. Reflecting at two parallel planes m, m' with distance $\mathbf{t}/2$ we get the so-called *translator* (*translation operator* by \mathbf{t})

$$X' = m'mXmm' = T_{\mathbf{t}}^{-1}XT_{\mathbf{t}}, \quad T_{\mathbf{t}} = 1 + \frac{1}{2}\mathbf{t}\mathbf{e}_{\infty}. \quad (2.21)$$

Reflection at two non-parallel planes m, m' yields the rotation around the m, m' -intersection line axis by twice the angle subtended by m, m' .

Group theoretically the conformal group $C(3)$ is isomorphic to $O(4, 1)$ and the Euclidean group $E(3)$ is the subgroup of $O(4, 1)$ leaving infinity \mathbf{e}_{∞} invariant [11, 12, 25]. Now general translations and rotations are represented by geometric products of vectors. To study combinations of versors it is useful to know that (cf. Table 3)

$$T_{\mathbf{t}} \mathbf{a} = \mathbf{a} T_{\mathbf{t}'}, \quad \mathbf{t}' = -\mathbf{a}^{-1} \mathbf{t} \mathbf{a}. \quad (2.22)$$

Applying these techniques one can compactly tabulate geometric space group symbols and generators [12]. Table 4 implements this for the 13 monoclinic space groups. All this is interactively visualized [16] by the Space Group Visualizer [31].

3. Subperiodic groups represented in Clifford's geometric algebra

Now we begin to explain the details of the new geometric algebra based representation of so-called *subperiodic* space groups. These include the seven *frieze* groups (in 2D space, 1 degree of freedom (DOF) for translation), the 75 *rod* groups (in 3D space, 1 DOF for translation), and the 80 *layer* groups (in 3D space, 2 DOF for translations).

Compared to the geometric 2D and 3D space group symbols in [12] we have introduced dots: If one or two dots occur between the Bravais symbol (\mathcal{P} , p , c) and index 1, the vector \mathbf{b} or \mathbf{c} , respectively, is present in the generator list. If one or two dots appear between the Bravais symbol and the index 2 (without or with bar), then the vectors \mathbf{b}, \mathbf{c} or \mathbf{a}, \mathbf{c} , respectively, are present in the generator list.

In agreement [12] the indexes a, b, c, n (and g for frieze groups) in first, second or third position after the Bravais symbol indicate that the reflections $\mathbf{a}, \mathbf{b}, \mathbf{c}$ (in this order) become glide reflections. An index n indicates diagonal glides. The dots also serve as symbolic a, b, c position indicators. For example rod group 5: $\mathcal{P}_c 1$ has glide reflection $\mathbf{a} T_{\mathbf{c}}^{1/2}$, rod group 19: $\mathcal{P}_{\bar{c}} 2$ has $\mathbf{b} T_{\mathbf{c}}^{1/2}$, and layer group 39: $p_b 2a 2_n$ has $\mathbf{a} T_{\mathbf{b}}^{\frac{1}{2}}$, $\mathbf{b} T_{\mathbf{a}}^{1/2}$ and $\mathbf{c} T_{\mathbf{a}+\mathbf{b}}^{1/2}$.

TABLE 4. Monoclinic space group versor generators, $T^A = T_{\mathbf{b}+\mathbf{c}}^{1/2}$, col. 1: international space group number [9], col. 2: international space group symbol [9], col. 3: geometric space group symbol [12], col. 4: geometric space group versor generators [12], cols. 5 and 6: alternative geometric space group versor generators [17]. The pure translators $T_{\mathbf{a}}, T_{\mathbf{b}}, T_{\mathbf{c}}$ are omitted.

1.	2.	3.	4.	5.	6.
3	$P2$	$P\bar{2}$	$i\mathbf{c} = \mathbf{a} \wedge \mathbf{b}$		
4	$P2_1$	$P\bar{2}_1$	$i\mathbf{c}T_{\mathbf{c}}^{1/2}$		
5	$C2$	$A\bar{2}$	$i\mathbf{c}, T^A$		
6	Pm	$P1$	\mathbf{c}		
7	Pc	P_a1	$\mathbf{c}T_{\mathbf{a}}^{1/2}$		
8	Cm	$A1$	\mathbf{c}, T^A		
9	Cc	A_a1	$\mathbf{c}T_{\mathbf{a}}^{1/2}, T^A$		
10	$P2/m$	$P2\bar{2}$	$\mathbf{c}, i\mathbf{c}$	$i, i\mathbf{c}$	i, \mathbf{c}
11	$P2_1/m$	$P2\bar{2}_1$	$\mathbf{c}, i\mathbf{c}T_{\mathbf{c}}^{1/2}$	$i, i\mathbf{c}T_{\mathbf{c}}^{1/2}$	$i, \mathbf{c}T_{\mathbf{c}}^{1/2}$
12	$C2/m$	$A2\bar{2}$	$\mathbf{c}, i\mathbf{c}, T^A$	$iT^A, i\mathbf{c}T^A, T^A$	i, \mathbf{c}, T^A
13	$P2/c$	$P_a2\bar{2}$	$\mathbf{c}T_{\mathbf{a}}^{1/2}, i\mathbf{c}$	$i, i\mathbf{c}T_{\mathbf{a}}^{1/2}$	$i, \mathbf{c}T_{\mathbf{a}}^{1/2}$
14	$P2_1/c$	$P_a2\bar{2}_1$	$\mathbf{c}T_{\mathbf{a}}^{1/2}, i\mathbf{c}T_{\mathbf{c}}^{1/2}$	$i, i\mathbf{c}T_{\mathbf{a}+\mathbf{c}}^{1/2}$	$i, \mathbf{c}T_{\mathbf{a}+\mathbf{c}}^{1/2}$
15	$C2/c$	$A_a2\bar{2}$	$\mathbf{c}T_{\mathbf{a}}^{1/2}, i\mathbf{c}, T^A$	$i, i\mathbf{c}T_{\mathbf{a}}^{1/2}, T^A$	$i, \mathbf{c}T_{\mathbf{a}}^{1/2}, T^A$

The notation \bar{n}_p indicates a right handed screw rotation of $2\pi/n$ around the \bar{n} -axis, with pitch $T_{\mathbf{t}}^{p/n}$ where \mathbf{t} is the shortest lattice translation vector parallel to the axis, in the screw direction. For example the layer group 21: $p\bar{2}\bar{2}_1\bar{2}_1$ has the screw generators $\mathbf{bc}T_{\mathbf{a}}^{1/2}$ and $\mathbf{ac}T_{\mathbf{b}}^{1/2}$.

In the following we discuss specific issues for frieze groups, rod groups and layer groups.

3.1. Frieze groups

Figure 5 shows the generating vectors \mathbf{a}, \mathbf{b} of oblique and rectangular cells for 2D frieze groups. The only translation direction is \mathbf{a} , frieze groups are thus subgroups of plane space groups, which can also be fully visualized with the interactive Space Group Visualizer software [20]. Table 5 lists the seven frieze groups with *new geometric symbols* and *generators*.

3.2. Rod groups

Figure 3 shows the generating vectors $\mathbf{a}, \mathbf{b}, \mathbf{c}$ of triclinic, monoclinic, orthorhombic and tetragonal cells for 3D rod and layer groups. Figure 4 shows the same for trigonal and hexagonal cells. For rod groups the only translation direction is \mathbf{c} . There is a total of 75 rod groups in all 3D crystal systems. Table 6 lists the triclinic, monoclinic and orthorhombic rod groups with *new geometric symbols* and *generators*:

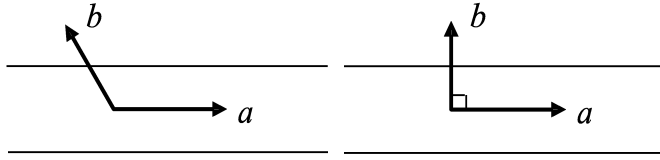


FIGURE 5. Generating vectors \mathbf{a}, \mathbf{b} of oblique and rectangular cells for 2D frieze groups.

Rod group number (col. 1), international rod group notation [23] (col. 2), international 3D space super group numbers [9] (col. 3), and notation [9] (col. 4), geometric 3D space super group notation [12] (col. 5), *geometric rod group notation* (col. 6), *geometric algebra generators* (col. 7). The tetragonal and trigonal rod groups are listed in Table 7, and the hexagonal rod groups in Table 8.

Note that in the last two rows of Table 7 we give in col. 5 the geometric 3D space super group notation exactly as found in [12]. But for full consistency with the choice of vectors in Table 2 and Fig. 4, we have decided to modify the rod group notation (and their versor generators) specified in col. 6 (and col. 7) of the last two rows of Table 7.

3.3. Layer groups

For layer groups the two translation directions are \mathbf{a}, \mathbf{b} . There is a total of 80 layer groups. Table 9 lists the triclinic and monoclinic 3D layer groups with new geometric symbols and generators: Layer group number (col. 1), international layer group notation³ [23] (col. 2), international 3D space super group numbers [9] (col. 3), and notation [9] (col. 4), geometric 3D space super group notation [12] (col. 5), *geometric layer group notation* (col. 6), *geometric algebra generators* (col. 7). Table 10 lists the orthorhombic/rectangular layer groups, and Table 11 the tetragonal/square, trigonal/hexagonal and hexagonal/hexagonal layer groups. The layer groups are classified according to their 3D crystal system/2D Bravais system⁴. The monoclinic/oblique (rectangular) system corresponds to the monoclinic/orthogonal (inclined) system of Fig. 3. Figure 4 shows the hexagonally centered cell with Bravais symbols H (space group) and h (layer group).

Note that we use in Table 11 for the symmorphic space group No. 81 the rotary reflection generator \mathbf{abc} and not \mathbf{bac} of Table 5 of [12]. But the point groups and symmorphic space groups generated by \mathbf{abc} and \mathbf{bac} are the same, because for $p = 4$ we have the following equalities (up to non-zero scalar factors, which cancel out in (2.11))

$$\mathbf{ba} \doteq (\mathbf{ab})^3, \quad (\mathbf{ba})^2 \doteq (\mathbf{ab})^2, \quad (\mathbf{ba})^3 \doteq \mathbf{ab}, \quad (3.1)$$

and hence with $q = 2$, $\mathbf{bac} = \mathbf{cba}$, $\mathbf{abc} = \mathbf{cab}$, and $\mathbf{c}^2 \doteq 1$ we also have

$$\mathbf{bac} \doteq (\mathbf{abc})^3, \quad (\mathbf{bac})^2 \doteq (\mathbf{abc})^2, \quad (\mathbf{bac})^3 \doteq \mathbf{abc}. \quad (3.2)$$

³Further well known and used layer group symbols are due to Wood, and to Bohm and Dornberger-Schiff [24].

⁴Note that *Bravais systems* have officially been renamed *lattice systems* since 2002.

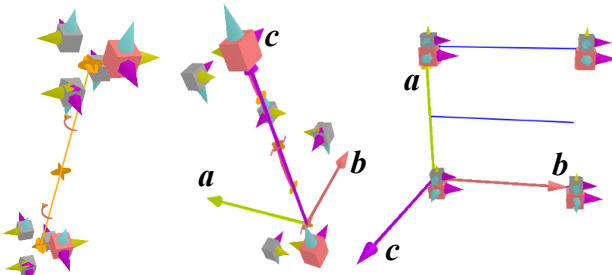


FIGURE 6. How a future subperiodic space group viewer software might depict rod groups 13: $\bar{2}\bar{2}\bar{2}$ and 14: $\bar{2}_1\bar{2}\bar{2}$, and the layer group 11: $p1$, based on citeHP:TheSGV.

That is, the two sets of point transformations generated by the integer powers of the generators **abc** and **bac** are identical for $p = 4, q = 2$. We have therefore decided for consistency with Table 2, to use for the space group No. 81 the geometric symbol $P\bar{4}2$ and the generator **abc**. A similar argument is valid for our use of the generator **abc** for space group No. 147 in our Table 11, instead of **bac** in Table 5 of [12].

4. Conclusion

We have devised a new representation for the 162 subperiodic space groups in Clifford's geometric algebra using versors (Clifford monomials, Lipschitz elements). In the future this may be extended to magnetic subperiodic space groups. We expect that the present work forms a suitable foundation for interactive visualization software of subperiodic space groups [16]. Fig. 6 shows how the rod groups 13: $\bar{2}\bar{2}\bar{2}$ and 14: $\bar{2}_1\bar{2}\bar{2}$, and the layer group 11: $p1$ might be visualized in the future, based on [16].

Acknowledgment

E. Hitzer wishes to thank God for his wonderful creation: *You answer us with awesome deeds of righteousness, O God our Savior, the hope of all the ends of the earth and of the farthest seas ...* [39]. He wishes to thank his family for their loving support, and D. Hestenes, C. Perwass, M. Aroyo, D. Litvin, A. Hayashi, N. Onoda, Y. Koga, H. Zimmermann and the anonymous reviewers. We particularly thank one of the reviewers for pointing out references [32–34, 36–38].

References

- [1] E. Cartan, *La Théorie des Spineurs I, II.*, Actualités Scientifiques et Industrielles, No. 643. Paris: Hermann, 1938
- [2] W.K. Clifford, *Applications of Grassmann's extensive algebra*, American Journal of Mathematics Pure and Applied 1, pp. 350–358 (1878).

TABLE 5. Table of frieze groups. Group number (col. 1), international frieze group notation [23] (col. 2), international 3D space super group numbers [9] (col. 3), and notation [9] (col. 4), geometric 3D space super group notation [12] (col. 5), international 2D space super group numbers [9] (col. 6), and notation [9] (col. 7), geometric 2D space super group notation [12] (col. 8), *geometric frieze group notation* (col. 9), *geometric algebra frieze group verson generators* (col. 10). The pure translator $T_{\mathbf{a}}$ is omitted.

1.	2.	3.	4.	5.	6.	7.	8.	9.	10.
Oblique									
1	$\mathcal{A}1$	1	$P1$	$P\bar{1}$	1	$p1$	$p\bar{1}$	$\mathcal{A}\bar{1}$	
2	$\mathcal{A}211$	3	$P2$	$P\bar{2}$	2	$p2$	$p\bar{2}$	$\mathcal{A}\bar{2}$	$\mathbf{a} \wedge \mathbf{b}$
Rectangular									
3	$\mathcal{A}1m1$	6	Pm	$P1$	3	pm ($p1m1$)	$p1$	$\mathcal{A}1$	\mathbf{a}
4	$\mathcal{A}11m$	6	Pm	$P1$	3	pm ($p11m$)	$p1$	$\mathcal{A}1$	\mathbf{b}
5	$\mathcal{A}11g$	7	Pc	P_a1	4	pg ($p11g$)	p_g1	$\mathcal{A}g1$	$\mathbf{b}T_{\mathbf{a}}^{1/2}$
6	$\mathcal{A}2mm$	25	$Pmm2$	$P2$	6	$p2mm$	$p2$	$\mathcal{A}2$	\mathbf{a}, \mathbf{b}
7	$\mathcal{A}2mg$	28	$Pma2$	$P2_a$	7	$p2mg$	$p2_g$	$\mathcal{A}2_g$	$\mathbf{a}, \mathbf{b}T_{\mathbf{a}}^{1/2}$

- [3] H.S.M. Coxeter, *Discrete groups generated by reflections*, Ann. of Math. **35**, pp. 588–621, (1934).
- [4] H.S.M. Coxeter, W.O.J. Moser, *Generators and Relations for Discrete Groups*, 4th ed., Springer: New York, 1980.
- [5] J. Dieudonné, *Sur les Groupes Classiques*, Actualités Scientifiques et Industrielles, No. 1040, Hermann: Paris, 1948.
- [6] C. Doran, A. Lasenby, *Geometric Algebra for Physicists*, Cambridge University Press, Cambridge (UK), 2003.
- [7] L. Dorst, D. Fontijne, S. Mann, *Geometric Algebra for Computer Science: An Object-oriented Approach to Geometry*. Morgan Kaufmann Series in Computer Graphics: San Francisco, 2007.
- [8] J.D.M. Gutierrez, *Operaciones de simetría mediante álgebra geométrica aplicadas a grupos cristalográficos*, MSc thesis, UNAM, Mexico, 1996.
- [9] T. Hahn, *Int. Tables for Crystallography*, 5th ed., Vol. A., Wiley: Hoboken, 2005.
- [10] D. Hestenes, H. Li, A. Rockwood, *New Algebraic Tools for Classical Geometry*, in G. Sommer (ed.), *Geometric Computing with Clifford Algebras*, Springer: Basel, pp. 4–26, 2001.
- [11] D. Hestenes, *Point groups and space groups in geometric algebra*, edited by L. Dorst et al., *Applications of Geometric Algebra in Computer Science and Engineering*, Birkhäuser: Basel, pp. 3–34, 2002.
- [12] D. Hestenes, J. Holt, *The Crystallographic Space Groups in Geometric Algebra*, JMP, **48**, 023514, (2007).

TABLE 6. Table of triclinic, monoclinic and orthorhombic rod groups. The pure translator T_c is omitted.

1.	2.	3.	4.	5.	6.	7.
Triclinic						
1	$\mu 1$	1	$P\bar{1}$	$P\bar{1}\bar{2}$	$\mu \bar{1}\bar{2}$	
2	$\mu \bar{1}$	2	$P\bar{1}$	$P\bar{2}\bar{2}$	$\mu \bar{2}\bar{2}$	$\mathbf{a} \wedge \mathbf{b} \wedge \mathbf{c}$
Monoclinic/inclined						
3	$\mu 211$	3	$P112$	$P\bar{2}$	$\mu .\bar{2}$	$\mathbf{b} \wedge \mathbf{c}$
4	$\mu m11$	6	Pm	$P1$	$\mu 1$	\mathbf{a}
5	$\mu c11$	7	Pc	P_c1	μ_c1	$\mathbf{a}T_c^{1/2}$
6	$\mu 2/m11$	10	$P2/m$	$P2\bar{2}$	$\mu 2\bar{2}$	$\mathbf{a}, \mathbf{b} \wedge \mathbf{c}$
7	$\mu 2/c11$	13	$P2/c$	$P_a2\bar{2}$	$\mu_c2\bar{2}$	$\mathbf{a}T_c^{1/2}, \mathbf{b} \wedge \mathbf{c}$
Monoclinic/orthogonal						
8	$\mu 112$	3	$P112$	$P\bar{2}$	$\mu \bar{2}$	$\mathbf{a} \wedge \mathbf{b}$
9	$\mu 112_1$	4	$P2_1$	$P\bar{2}_1$	$\mu \bar{2}_1$	$(\mathbf{a} \wedge \mathbf{b})T_c^{1/2}$
10	$\mu 11m$	6	Pm	$P1$	$\mu ..1$	\mathbf{c}
11	$\mu 112/m$	10	$P2/m$	$P\bar{2}2$	$\mu \bar{2}2$	$\mathbf{a} \wedge \mathbf{b}, \mathbf{c}$
12	$\mu 112_1/m$	11	$P2_1/m$	$P\bar{2}_12$	$\mu \bar{2}_12$	$(\mathbf{a} \wedge \mathbf{b})T_c^{1/2}, \mathbf{c}$
Orthorhombic						
13	$\mu 222$	16	$P222$	$P\bar{2}\bar{2}\bar{2}$	$\mu \bar{2}\bar{2}\bar{2}$	\mathbf{ab}, \mathbf{bc}
14	$\mu 222_1$	17	$P222_1$	$P\bar{2}_1\bar{2}\bar{2}$	$\mu \bar{2}_1\bar{2}\bar{2}$	$\mathbf{ab}T_c^{1/2}, \mathbf{bc}$
15	$\mu mm2$	25	$Pmm2$	$P2$	$\mu 2$	\mathbf{a}, \mathbf{b}
16	$\mu cc2$	27	$Pcc2$	P_c2_c	μ_c2_c	$\mathbf{a}T_c^{1/2}, \mathbf{b}T_c^{1/2}$
17	$\mu mc2_1$	26	$Pmc2_1$	$P2_c$	$\mu 2_c$	$\mathbf{a}, \mathbf{b}T_c^{1/2}$
18	$\mu 2mm$	25	$Pmm2$	$P2$	$\mu .2$	\mathbf{b}, \mathbf{c}
19	$\mu 2cm$	28	$Pma2$	$P2_a$	$\mu .c2$	$\mathbf{b}T_c^{1/2}, \mathbf{c}$
20	μmmm	47	$Pmmm$	$P22$	$\mu 22$	$\mathbf{a}, \mathbf{b}, \mathbf{c}$
21	μccm	49	$Pccm$	P_c2_c2	μ_c2_c2	$\mathbf{a}T_c^{1/2}, \mathbf{b}T_c^{1/2}, \mathbf{c}$
22	μmcm	51	$Pmma$	$P22_a$	$\mu 2_c2$	$\mathbf{a}, \mathbf{b}T_c^{1/2}, \mathbf{c}$

- [13] E. Hitzer, *Euclidean Geometric Objects in the Clifford Geometric Algebra of {Origin, 3-Space, Infinity}*, Bull. of the Belg. Math. Soc. – Simon Stevin, Vol. 11, No. 5, pp. 653–662 (2004).
- [14] E. Hitzer, C. Perwass, *Crystal cells in geometric algebra*, in Proc. of Int. Symp. on Adv. Mech. Engrng. (ISAME 2004), University of Fukui, Japan, pp. 290–295, 2004.
- [15] E. Hitzer, C. Perwass, *Full Geometric Description of All Symmetry Elements of Crystal Space Groups by the Suitable Choice of Only Three Vectors for Each Bravais Cell or Crystal Family*, Proc. of ISAME 2005, Busan, South Korea, pp. 19–25, 2005.
- [16] E. Hitzer, C. Perwass *The Space Group Visualizer*, Proc. of ISAME 2006, USST, Shanghai, China, pp:172–181, 2006.

TABLE 7. Table of tetragonal and trigonal rod groups. The pure translator T_c is omitted.

1.	2.	3.	4.	5.	6.	7.
Tetragonal						
23	$\mu 4$	75	$P4$	$P\bar{4}$	$\mu \bar{4}$	ab
24	$\mu 4_1$	76	$P4_1$	$P\bar{4}_1$	$\mu \bar{4}_1$	$\text{ab}T_c^{\frac{1}{4}}$
25	$\mu 4_2$	77	$P4_2$	$P\bar{4}_2$	$\mu \bar{4}_2$	$\text{ab}T_c^{\frac{1}{2}}$
26	$\mu 4_3$	78	$P4_3$	$P\bar{4}_3$	$\mu \bar{4}_3$	$\text{ab}T_c^{\frac{3}{4}}$
27	$\mu \bar{4}$	81	$P\bar{4}$	$P\bar{4}\bar{2}$	$\mu \bar{4}\bar{2}$	abc
28	$\mu 4/m$	83	$P4/m$	$P\bar{4}2$	$\mu \bar{4}2$	ab, c
29	$\mu 4_2/m$	84	$P4_2/m$	$P\bar{4}_22$	$\mu \bar{4}_22$	$\text{ab}T_c^{\frac{1}{2}}, \text{c}$
30	$\mu 422$	89	$P422$	$P\bar{4}\bar{2}\bar{2}$	$\mu \bar{4}\bar{2}\bar{2}$	ab, bc
31	$\mu 4_{122}$	91	$P4_{122}$	$P\bar{4}_1\bar{2}\bar{2}$	$\mu \bar{4}_1\bar{2}\bar{2}$	$\text{ab}T_c^{\frac{1}{4}}, \text{bc}$
32	$\mu 4_{222}$	93	$P4_{222}$	$P\bar{4}_2\bar{2}\bar{2}$	$\mu \bar{4}_2\bar{2}\bar{2}$	$\text{ab}T_c^{\frac{1}{2}}, \text{bc}$
33	$\mu 4_{322}$	95	$P4_{322}$	$P\bar{4}_3\bar{2}\bar{2}$	$\mu \bar{4}_3\bar{2}\bar{2}$	$\text{ab}T_c^{\frac{3}{4}}, \text{bc}$
34	$\mu 4mm$	99	$P4mm$	$P4$	$\mu 4$	a, b
35	$\mu 4_{2cm}$	101	$P4_{2cm}$	P_c4	μ_c4	$\text{a}T_c^{\frac{1}{2}}, \text{b}$
36	$\mu 4cc$	103	$P4cc$	P_c4_c	μ_c4_c	$\text{a}T_c^{\frac{1}{2}}, \text{b}T_c^{\frac{1}{2}}$
37	$\mu \bar{4}m2$	115	$P\bar{4}m2$	$P4\bar{2}$	$\mu 4\bar{2}$	a, bc
38	$\mu \bar{4}c2$	116	$P\bar{4}c2$	$P_c4\bar{2}$	$\mu_c4\bar{2}$	$\text{a}T_c^{\frac{1}{2}}, \text{bc}$
39	$\mu 4/mmm$	123	$P4/mmm$	$P42$	$\mu 42$	a, b, c
40	$\mu 4/mcc$	124	$P4/mcc$	P_c4_c2	μ_c4_c2	$\text{a}T_c^{\frac{1}{2}}, \text{b}T_c^{\frac{1}{2}}, \text{c}$
41	$\mu 4_2/mmc$	131	$P4_2/mmc$	$P4_c2$	$\mu 4_c2$	a, b $T_c^{\frac{1}{2}}, \text{c}$
Trigonal						
42	$\mu 3$	143	$P3$	$P\bar{3}$	$\mu \bar{3}$	ab
43	$\mu 3_1$	144	$P3_1$	$P\bar{3}_1$	$\mu \bar{3}_1$	$\text{ab}T_c^{\frac{1}{3}}$
44	$\mu 3_2$	145	$P3_2$	$P\bar{3}_2$	$\mu \bar{3}_2$	$\text{ab}T_c^{\frac{2}{3}}$
45	$\mu \bar{3}$	147	$P\bar{3}$	$P\bar{6}2$	$\mu 6\bar{2}$	abc
46	$\mu 312$	149	$P312$	$P\bar{3}\bar{2}$	$\mu \bar{3}\bar{2}$	ab, bc
47	$\mu 3_{12}$	151	$P3_{12}$	$P\bar{3}_1\bar{2}$	$\mu \bar{3}_1\bar{2}$	$\text{ab}T_c^{\frac{1}{3}}, \text{bc}$
48	$\mu 3_{212}$	153	$P3_{212}$	$P\bar{3}_2\bar{2}$	$\mu \bar{3}_2\bar{2}$	$\text{ab}T_c^{\frac{2}{3}}, \text{bc}$
49	$\mu 3m1$	156	$P3m1$	$P3$	$\mu 3$	a, b
50	$\mu 3c1$	158	$P3c1$	P_c3_c	μ_c3_c	$\text{a}T_c^{\frac{1}{2}}, \text{b}T_c^{\frac{1}{2}}$
51	$\mu \bar{3}1m$	162	$P\bar{3}1m$	$P\bar{2}6$	$\mu 6\bar{2}$	a, bc
52	$\mu \bar{3}1c$	163	$P\bar{3}1c$	$P\bar{2}_c6$	$\mu_c6\bar{2}$	$\text{a}T_c^{\frac{1}{2}}, \text{bc}$

[17] E. Hitzer, C. Perwass. *Three Vector Generation of Crystal Space Groups in Geometric Algebra*, Bulletin of the Society for Science on Form, **21**(1), pp. 55–56 (2006).

TABLE 8. Table of hexagonal rod groups. The pure translator T_c is omitted.

1.	2.	3.	4.	5.	6.	7.
53	$\not{6}$	168	$P6$	$P\bar{6}$	$\not{\bar{6}}$	ab
54	$\not{6}_1$	169	$P6_1$	$P\bar{6}_1$	$\not{\bar{6}}_1$	$abT_c^{\frac{1}{6}}$
55	$\not{6}_2$	171	$P6_2$	$P\bar{6}_2$	$\not{\bar{6}}_2$	$abT_c^{\frac{1}{3}}$
56	$\not{6}_3$	173	$P6_3$	$P\bar{6}_3$	$\not{\bar{6}}_3$	$abT_c^{\frac{1}{2}}$
57	$\not{6}_4$	172	$P6_4$	$P\bar{6}_4$	$\not{\bar{6}}_4$	$abT_c^{\frac{2}{3}}$
58	$\not{6}_5$	170	$P6_5$	$P\bar{6}_5$	$\not{\bar{6}}_5$	$abT_c^{\frac{5}{6}}$
59	$\not{\bar{6}}$	174	$P\bar{6}$	$P\bar{3}2$	$\not{\bar{3}}2$	ab, c
60	$\not{6}/m$	175	$P6/m$	$P\bar{6}2$	$\not{\bar{6}}2$	ab, c
61	$\not{6}_3/m$	176	$P6_3/m$	$P\bar{6}_32$	$\not{\bar{6}}_32$	$abT_c^{\frac{1}{2}}, c$
62	$\not{6}_{22}$	177	$P6_{22}$	$P\bar{6}\bar{2}$	$\not{\bar{6}}\bar{2}$	ab, bc
63	$\not{6}_122$	178	$P6_122$	$P\bar{6}_1\bar{2}$	$\not{\bar{6}}_1\bar{2}$	$abT_c^{\frac{1}{6}}, bc$
64	$\not{6}_{222}$	180	$P6_{222}$	$P\bar{6}_2\bar{2}$	$\not{\bar{6}}_2\bar{2}$	$abT_c^{\frac{1}{3}}, bc$
65	$\not{6}_322$	182	$P6_322$	$P\bar{6}_3\bar{2}$	$\not{\bar{6}}_3\bar{2}$	$abT_c^{\frac{1}{2}}, bc$
66	$\not{6}_{422}$	181	$P6_{422}$	$P\bar{6}_4\bar{2}$	$\not{\bar{6}}_4\bar{2}$	$abT_c^{\frac{2}{3}}, bc$
67	$\not{6}_522$	179	$P6_522$	$P\bar{6}_5\bar{2}$	$\not{\bar{6}}_5\bar{2}$	$abT_c^{\frac{5}{6}}, bc$
68	$\not{6}mm$	183	$P6mm$	$P6$	$\not{6}$	a, b
69	$\not{6}cc$	184	$P6cc$	P_c6_c	$\not{c}6_c$	$aT_c^{\frac{1}{2}}, bT_c^{\frac{1}{2}}$
70	$\not{6}_3cm$	185	$P6_3cm$	P_c6	$\not{c}6$	$aT_c^{\frac{1}{2}}, b$
71	$\not{\bar{6}}m2$	187	$P\bar{6}m2$	$P32$	$\not{3}2$	a, b, c
72	$\not{\bar{6}}c2$	188	$P\bar{6}c2$	P_c3_c2	$\not{c}3_c2$	$aT_c^{\frac{1}{2}}, bT_c^{\frac{1}{2}}, c$
73	$\not{6}/mmm$	191	$P6/mmm$	$P62$	$\not{6}2$	a, b, c
74	$\not{6}/mcc$	192	$P6/mcc$	P_c6_c2	$\not{c}6_c2$	$aT_c^{\frac{1}{2}}, bT_c^{\frac{1}{2}}, c$
75	$\not{6}_3/mcm$	193	$P6_3/mcm$	P_c62	$\not{c}62$	$aT_c^{\frac{1}{2}}, b, c$

- [18] E. Hitzer, C. Perwass, *Interactive 3D Space Group Visualization with CLUCalc and the Clifford Geometric Algebra Description of Space Groups*, Adv. Appl. Clifford Alg., Vol. 20(3-4), pp. 631–658, (2010), DOI 10.1007/s00006-010-0214-z.
- [19] E. Hitzer, C. Perwass, D. Ichikawa, *Interactive 3D Space Group Visualization with CLUCalc and Crystallographic Subperiodic Groups in Geometric Algebra*, in G. Scheuermann, E. Bayro-Corchozano (eds.), Geometric Algebra Computing, Springer, New York, 2010, pp. 385–400.
- [20] E. Hitzer, *Interactive visualization of plane groups*, in G. Lugosi, D. Nagy (eds.), Symmetry: Art and Science, Spec. Iss. of The Journal of the Int. Soc. For the Interdisc. Study of Symmetry (ISIS): Proc. of Symmetry: Art and Science, 8th Congress of ISIS, Days of Harmonics, Gmund, Austria, 23–28 Aug. 2010, Vol. 2010 (1-4), pp. 80–83, (2010).
- [21] E. Hitzer, K. Tachibana, S. Buchholz, and I. Yu, *Carrier Method for the General Evaluation and Control of Pose, Molecular Conformation, Tracking, and the Like*, Adv. Appl. Clifford Alg., Vol. 19, No. 2, pp. 339–364 (2009).

TABLE 9. Table of triclinic and monoclinic layer groups. The pure translators $T_{\mathbf{a}}, T_{\mathbf{b}}$ are omitted.

1.	2.	3.	4.	5.	6.	7.
Triclinic/oblique						
1	$p1$	1	$P1$	$P\bar{1}$	$p\bar{1}$	
2	$p\bar{1}$	2	$P\bar{1}$	$P\bar{2}\bar{2}$	$p\bar{2}\bar{2}$	$\mathbf{a} \wedge \mathbf{b} \wedge \mathbf{c}$
Monoclinic/oblique						
3	$p112$	3	$P2$	$P\bar{2}$	$p\bar{2}$	$\mathbf{a} \wedge \mathbf{b}$
4	$p11m$	6	Pm	$P1$	$p..1$	\mathbf{c}
5	$p11a$	7	Pc	P_a1	$p_{..a}1$	$\mathbf{c}T_a^{\frac{1}{2}}$
6	$p112/m$	10	$P2/m$	$P\bar{2}2$	$p\bar{2}2$	$\mathbf{a} \wedge \mathbf{b}, \mathbf{c}$
7	$p112/a$	13	$P2/c$	$P_a2\bar{2}$	$p\bar{2}2_a$	$\mathbf{a} \wedge \mathbf{b}, \mathbf{c}T_a^{\frac{1}{2}}$
Monoclinic/rectangular						
8	$p211$	3	$P2$	$P\bar{2}$	$p.\bar{2}$	$\mathbf{b} \wedge \mathbf{c}$
9	$p2111$	4	$P2_1$	$P\bar{2}_1$	$p.\bar{2}_1$	$(\mathbf{b} \wedge \mathbf{c})T_a^{\frac{1}{2}}$
10	$c211$	5	$C2$	$A\bar{2}$	$c.\bar{2}$	$\mathbf{b} \wedge \mathbf{c}, T_{\mathbf{a}+\mathbf{b}}^{1/2}$
11	$pm11$	6	Pm	$P1$	$p1$	\mathbf{a}
12	$pb11$	7	Pc	P_a1	p_b1	$\mathbf{a}T_b^{\frac{1}{2}}$
13	$cm11$	8	Cm	$A1$	$c1$	$\mathbf{a}, T_{\mathbf{a}+\mathbf{b}}^{1/2}$
14	$p2/m11$	10	$P2/m$	$P2\bar{2}$	$p2\bar{2}$	$\mathbf{a}, \mathbf{b} \wedge \mathbf{c}$
15	$p2_1/m11$	11	$P2_1/m$	$P2\bar{2}_1$	$p2\bar{2}_1$	$\mathbf{a}, (\mathbf{b} \wedge \mathbf{c})T_a^{\frac{1}{2}}$
16	$p2/b11$	13	$P2/c$	$P_a2\bar{2}$	$p_b2\bar{2}$	$\mathbf{a}T_b^{\frac{1}{2}}, \mathbf{b} \wedge \mathbf{c}$
17	$p2_1/b11$	14	$P2_1/c$	$P_a2\bar{2}_2$	$p_b2\bar{2}_1$	$\mathbf{a}T_b^{\frac{1}{2}}, (\mathbf{b} \wedge \mathbf{c})T_a^{\frac{1}{2}}$
18	$c2/m11$	12	$C2/m$	$A\bar{2}\bar{2}$	$c2\bar{2}$	$\mathbf{a}, \mathbf{b} \wedge \mathbf{c}, T_{\mathbf{a}+\mathbf{b}}^{1/2}$

- [22] D. Ichikawa, E. Hitzer, *Symmetry of orthorhombic materials and interactive 3D visualization in Geometric Algebra*, Proc. of ISAMPE 2007, University of Fukui, Japan, pp. 302–312, 2007.
- [23] V. Kopsky, D.B. Litvin (eds.), *Int. Tables for Crystallography*, 1st ed., Vol. E, Springer: New York, 2002.
- [24] V. Kopsky, D.B. Litvin, *Nomenclature, Symbols and Classification of the Subperiodic Groups – Report of a Working Group of the International Union of Crystallography (IUCr) Commission on Crystallographic Nomenclature*, Presented To: Commission on Crystallographic Nomenclature of the International Union of Crystallography, *Acta Cryst. A49*, p. 594 (1993). Also available at www.bk.psu.edu/faculty/litvin/Download/D_IUCr_Report.pdf. Full final version in [23].
- [25] H. Li, *Invariant Algebras and Geometric Reasoning*, World Scientific: Singapore, 2008.
- [26] S. Lie, *On a class of geometric transformations*, PhD. thesis, University of Oslo, Oslo, Norway, 1872.
- [27] P. Lounesto, *Clifford Algebras and Spinors*, 2nd ed. Cambridge University Press: Cambridge (UK), 2001.

TABLE 10. Table of orthorhombic/rectangular layer groups. The pure translators $T_{\mathbf{a}}, T_{\mathbf{b}}$ are omitted.

1.	2.	3.	4.	5.	6.	7.
19	$p222$	16	$P222$	$P\bar{2}\bar{2}\bar{2}$	$p\bar{2}\bar{2}\bar{2}$	ab, bc
20	$p2_122$	17	$P222_1$	$P\bar{2}_1\bar{2}\bar{2}$	$p\bar{2}\bar{2}_1\bar{2}$	ab, bc $T_{\mathbf{a}}^{\frac{1}{2}}$
21	$p2_12_12$	18	$P2_12_12$	$P\bar{2}_1\bar{2}_1\bar{2}$	$p\bar{2}\bar{2}_1\bar{2}_1$	bc $T_{\mathbf{a}}^{\frac{1}{2}}$, ac $T_{\mathbf{b}}^{\frac{1}{2}}$
22	$c222$	21	$C222$	$C\bar{2}\bar{2}\bar{2}$	$c\bar{2}\bar{2}\bar{2}$	ab, bc, $T_{\mathbf{a}+\mathbf{b}}^{\frac{1}{2}}$
23	$pmm2$	25	$Pmm2$	$P2$	$p2$	a, b
24	$pma2$	28	$Pma2$	$P2_a$	$p2_a$	a, b $T_{\mathbf{a}}^{\frac{1}{2}}$
25	$pba2$	32	$Pba2$	P_b2_a	p_b2_a	a $T_{\mathbf{b}}^{\frac{1}{2}}$, b $T_{\mathbf{a}}^{\frac{1}{2}}$
26	$cmm2$	35	$Cmm2$	$C2$	$c2$	a, b, $T_{\mathbf{a}+\mathbf{b}}^{1/2}$
27	$pm2m$	25	$Pmm2$	$P2$	$p..2$	a, c
28	$pm2_1b$	26	$Pmc2_1$	$P2_c$	$p..b2$	a, c $T_{\mathbf{b}}^{\frac{1}{2}}$
29	$pb2_1m$	26	$Pmc2_1$	$P2_c$	$p_b..2$	a $T_{\mathbf{b}}^{\frac{1}{2}}$, c
30	$pb2b$	27	$Pcc2$	P_c2_c	$p_b..b2$	a $T_{\mathbf{b}}^{\frac{1}{2}}$, c $T_{\mathbf{b}}^{\frac{1}{2}}$
31	$pm2a$	28	$Pma2$	$P2_a$	$p..a2$	a, c $T_{\mathbf{a}}^{\frac{1}{2}}$
32	$pm2_1n$	31	$Pmn2_1$	$P2_n$	$p..n2$	a, c $T_{\mathbf{a}+\mathbf{b}}^{1/2}$
33	$pb2_1a$	29	$Pca2_1$	P_c2_a	$p_b..a2$	a $T_{\mathbf{b}}^{\frac{1}{2}}$, c $T_{\mathbf{a}}^{\frac{1}{2}}$
34	$pb2n$	30	$Pnc2$	P_n2_c	$p_b..n2$	a $T_{\mathbf{b}}^{\frac{1}{2}}$, c $T_{\mathbf{a}+\mathbf{b}}^{1/2}$
35	$cm2m$	35	$Cmm2$	$C2$	$c..2$	a, c, $T_{\mathbf{a}+\mathbf{b}}^{1/2}$
36	$cm2e$	39	$Aem2$	A_b2	$c..a2$	a, c $T_{\mathbf{a}}^{\frac{1}{2}}$, $T_{\mathbf{a}+\mathbf{b}}^{1/2}$
37	$pmmm$	47	$Pmmm$	$P22$	$p22$	a, b, c
38	$pmaa$	49	$Pccm$	P_c2_c2	$p2_a2_a$	a, b $T_{\mathbf{a}}^{\frac{1}{2}}$, c $T_{\mathbf{a}}^{\frac{1}{2}}$
39	$pban$	50	$Pban$	$P_b2_a2_n$	$p_b2_a2_n$	a $T_{\mathbf{b}}^{\frac{1}{2}}$, b $T_{\mathbf{a}}^{1/2}$, c $T_{\mathbf{a}+\mathbf{b}}^{-1/2}$
40	$pmam$	51	$Pmma$	$P22_a$	$p2_a2$	a, b $T_{\mathbf{a}}^{\frac{1}{2}}$, c
41	$pmma$	51	$Pmma$	$P22_a$	$p22_a$	a, b, c $T_{\mathbf{a}}^{\frac{1}{2}}$
42	$pman$	53	$Pmna$	$P2_n2_a$	$p2_a2_n$	a, b $T_{\mathbf{a}}^{\frac{1}{2}}$, c $T_{\mathbf{a}+\mathbf{b}}^{1/2}$
43	$pbaa$	54	$Pcca$	$P_c2_c2_a$	$p_b2_a2_a$	a $T_{\mathbf{b}}^{\frac{1}{2}}$, b $T_{\mathbf{a}}^{\frac{1}{2}}$, c $T_{\mathbf{a}}^{\frac{1}{2}}$
44	$pbam$	55	$Pbam$	P_b2_a2	p_b2_a2	a $T_{\mathbf{b}}^{\frac{1}{2}}$, b $T_{\mathbf{a}}^{\frac{1}{2}}$, c
45	$pbma$	57	$Pbcm$	P_b2_c2	p_b22_a	a $T_{\mathbf{b}}^{\frac{1}{2}}$, b , c $T_{\mathbf{a}}^{\frac{1}{2}}$
46	$pmmn$	59	$Pmmn$	$P22_n$	$p22_n$	a, b, c $T_{\mathbf{a}+\mathbf{b}}^{\frac{1}{2}}$
47	$cmmm$	65	$Cmmm$	$C22$	$c22$	a, b, c, $T_{\mathbf{a}+\mathbf{b}}^{1/2}$
48	$cmme$	67	$Cmme$	$C22_a$	$c22_a$	a, b, c $T_{\mathbf{a}}^{\frac{1}{2}}$, $T_{\mathbf{a}+\mathbf{b}}^{1/2}$

- [28] P. Lounesto, E. Latvamaa, *Conformal Transformations and Clifford Algebras*, Proc. of The AMS, Vol. 79, No. 4, pp. 533–538 (1980).
- [29] C. Perwass, *CLUCalc - Interactive Visualization software*, www.clucalc.info, 2002.
- [30] C. Perwass, E. Hitzer, *Interactive Visualization of Full Geometric Description of Crystal Space Groups*, Proc. of ISAME 2005, Busan, South Korea, pp. 276–282.

TABLE 11. Table of tetragonal, trigonal and hexagonal layer groups. Layer groups 57, 58 and 71 use special vector notation. The pure translators T_a, T_b are omitted.

1.	2.	3.	4.	5.	6.	7.
Tetragonal/square						
49	$p4$	75	$P4$	$\bar{P}4$	$p\bar{4}$	ab
50	$p\bar{4}$	81	$P\bar{4}$	$\bar{P}4\bar{2}$	$p4\bar{2}$	abc
51	$p4/m$	83	$P4/m$	$\bar{P}4\bar{2}$	$p\bar{4}\bar{2}$	ab, c
52	$p4/n$	85	$P4/n$	$\bar{P}4_n2$	$p\bar{4}_n2$	ab, $cT_b^{\frac{1}{2}}$
53	$p422$	89	$P422$	$\bar{P}4\bar{2}\bar{2}$	$p\bar{4}\bar{2}\bar{2}$	ab, bc
54	$p42_12$	90	$P4_212$	$\bar{P}4\bar{2}_1\bar{2}$	$p\bar{4}_2\bar{1}\bar{2}$	ab, $bcT_{2a-b}^{1/2}$
55	$p4mm$	99	$P4mm$	$P4$	$p4$	a, b
56	$p4bm$	100	$P4bm$	P_b4	p_b4	$aT_{a-b}^{1/2}, b$
57	$p\bar{4}2m$	111	$P\bar{4}2m$	$P\bar{2}4$	$p\bar{2}4$	ac, b
58	$p\bar{4}2_1m$	113	$P\bar{4}_21m$	$P\bar{2}_14$	$p\bar{2}_14$	$acT_{a-b}^{1/2}, b$
59	$p\bar{4}m2$	115	$P\bar{4}m2$	$P4\bar{2}$	$p4\bar{2}$	a, bc
60	$p\bar{4}b2$	117	$P\bar{4}b2$	$P_b4\bar{2}$	$p_b4\bar{2}$	$aT_{a-b}^{1/2}, bc$
61	$p4/mmm$	123	$P4/mmm$	$P42$	$p42$	a, b, c
62	$p4/nbm$	125	$P4/nbm$	P_b42_n	p_b42_n	$aT_{a-b}^{1/2}, b, cT_b^{\frac{1}{2}}$
63	$p4/mbm$	127	$P4/mbm$	P_b42	p_b42	$aT_{a-b}^{1/2}, b, c$
64	$p4/nmm$	129	$P4/nmm$	$P42_n$	$p42_n$	a, b, $cT_b^{\frac{1}{2}}$
Trigonal/hexagonal						
65	$p3$	143	$P3$	$P\bar{3}$	$p\bar{3}$	ab
66	$p\bar{3}$	147	$P\bar{3}$	$P\bar{6}\bar{2}$	$p\bar{6}\bar{2}$	abc
67	$p312$	149	$P312$	$P\bar{3}\bar{2}$	$p\bar{3}\bar{2}$	ab, bc
68	$p321$	150	$P321$	$H\bar{3}\bar{2}$	$h\bar{3}\bar{2}$	ab, bc
69	$p3m1$	156	$P3m1$	$P3$	$p3$	a, b
70	$p31m$	157	$P31m$	$H3$	$h3$	a, b
71	$p\bar{3}1m$	162	$P\bar{3}1m$	$P\bar{2}6$	$p\bar{2}6$	ac, b
72	$p\bar{3}m1$	164	$P\bar{3}m1$	$P6\bar{2}$	$p6\bar{2}$	a, bc
Hexagonal/hexagonal						
73	$p6$	168	$P6$	$P\bar{6}$	$p\bar{6}$	ab
74	$p\bar{6}$	174	$P\bar{6}$	$P\bar{3}2$	$p\bar{3}2$	ab, c
75	$p6/m$	175	$P6/m$	$P\bar{6}2$	$p\bar{6}2$	ab, c
76	$p622$	177	$P622$	$P\bar{6}\bar{2}$	$p\bar{6}\bar{2}$	ab, bc
77	$p6mm$	183	$P6mm$	$P6$	$p6$	a, b
78	$p\bar{6}m2$	187	$P\bar{6}m2$	$P32$	$p32$	a, b, c
79	$p\bar{6}2m$	189	$P\bar{6}2m$	$H32$	$h32$	a, b, c
80	$p6/mmm$	191	$P6/mmm$	$P62$	$p62$	a, b, c

- [31] C. Perwass, E. Hitzer, *Space Group Visualizer*, www.spacegroup.info, 2005.
- [32] M. A. Rodríguez, J. L. Aragón and L. Verde-Star, *Clifford algebra approach to the coincidence problem for planar lattices*, Acta Cryst. A61, pp. 173–184 (2005).
- [33] M. A. Rodríguez-Andrade, G. Aragón-González, J. L. Aragón and A. Gómez-Rodríguez, *Coincidence lattices in the hyperbolic plane*, Acta Cryst. A67, pp. 35–44 (2011).
- [34] M.A. Rodríguez-Andrade, G. Aragón-González, J.L. Aragón and L. Verde-Star, *An algorithm for the Cartana-Dieudonné theorem on generalized scalar product spaces*, Linear Algebra and its Applications, Vol. 434, Iss. 5, pp. 1238–1254, (2011).
- [35] B. Souvignier *Space Groups*, Syllabus for MaThCryst summer school, 15–20 July 2007, Havanna, Cuba.
- [36] F. Uhlig, *Constructive ways for generating (generalized) real orthogonal matrices as products of (generalized) symmetries*, Linear Algebra Appl., Vol. 332–334, pp. 459–467 (2001).
- [37] Y. M. Zou, *Structures of coincidence symmetry groups*, Acta Cryst. A62, pp. 109–114 (2006).
- [38] Y. M. Zou, *Indices of coincidence isometries of the hypercubic lattice* Acta Cryst. A62, pp. 454–458 (2006).
- [39] *The Holy Bible, New Int. Version*, Int. Bible Society: Colorado Springs, 1984.

Eckhard Hitzer

College of Liberal Arts, Department of Material Science,
International Christian University,
181-8585 Tokyo, Japan
e-mail: hitzer@icu.ac.jp

Daisuke Ichikawa

Department of Applied Physics,
University of Fukui,
910-8507 Fukui, Japan
e-mail: seiunnedved3032@yahoo.co.jp